

Measuring Ground Subsidence Rate in Bulacan and Pampanga Delta using Geodetic Techniques

Rosalie Reyes¹, Philip Minderhoud², John Dave Maclang¹, Alexi Mae Narca¹

¹ Department of Geodetic Engineering, University of the Philippines Diliman, Quezon City, Philippines – (rbreyes3, jmaclang, aynarca)@up.edu.ph

² Wageningen University, The Netherlands - philip.minderhoud@wur.nl

Keywords: land subsidence, GNSS, geodetic levelling, delta area, interferometry, vertical deformation, PSInSAR

Abstract

Based on the map produced from Sentinel-1 images using Permanent Scatterer Interferometric Synthetic Aperture Radar (PSInSAR), the Pampanga River basin is undergoing ground subsidence. Ground measurements using geodetic techniques such as differential levelling and Global Navigation Satellite System (GNSS) levelling can validate the deformation map. Several ground control points (GCPs) established previously were re-occupied by GNSS receivers. The results indicate similar trend i.e. land subsiding. Only 3 BMs were found in Bulacan and were given new elevations during the levelling campaign in 2021. The differences of the old and new values also indicate downtrend. Six (6) low-cost GNSS monitoring stations were installed in areas where subsidence rates are high based on the SAR deformation map to monitor the ongoing land subsidence. The initial results from 4 out of 6 GNSS monitoring stations for the 3-month observations showed a downtrend indicating land subsidence is occurring in the area.

1. Introduction

1.1 Background

In 2021, the mapping component of the Copernicus Emergency Management Service (EMS) provided evidence of ground motion patterns in the Pampanga River basin and Manila area using Sentinel-1 multi-temporal satellite SAR data analysis by persistent scatterers interferometry (PSInSAR) (EC and JRC, 2021). The deformation map shown in Figure 1 indicates that most of the delta area are undergoing land subsidence (red areas) with rates $> 50\text{mm/yr}$.

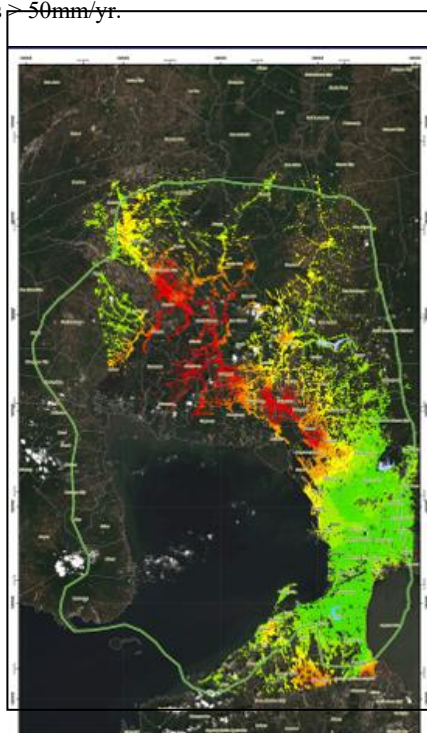


Figure 1. Deformation map in Pampanga River Basin and Manila North Area.

The Coastal Sea Level Rise (CSLR) Project determined vertical deformation using PSInSAR on selected coastal areas in the country. Based on the analysis most of the areas near the coast are undergoing land subsidence (Reyes et al., 2021). Notable is Cagayan de Oro and El Nido at -7mm/yr and -6mm/yr , respectively. Around 80% of the reference stations near the coasts from NAMRIA Active Geodetic Network analysed for vertical deformation are also exhibiting a downward trend (Ibid.). Most of these areas are in river deltas. This is the case for the Pampanga River delta that also covers not only the coastal barangays in Pampanga but also in Bulacan.

As spaced-based radar measurements are subject to some biases/errors due to signal propagation in the atmosphere, this introduced some errors in the results as well. The derived line-of sight (LOS) velocity rates from SAR processing can have an uncertainty ranging from 5 to 8 mm/yr measured against GNSS data (Casu et al., 2006; Duan et al., 2020; Cigna et al., 2020). However, this uncertainty is site specific because of other environmental factors affecting the SAR signal. Thus, it is necessary to validate the processed SAR map with in-situ geodetic measurements such as differential levelling and Global Navigation Satellite System (GNSS) levelling. These types of measurements are quite important as these have high accuracy. Importantly, residents easily accept the results from these techniques because they can see them being done on ground and therefore in terms of acceptability these are trustful enough. This is unlike space-based measurements that is hard for them to understand.

The purpose of this study is to quantify the land subsidence rates in the delta area through ground measurements using geodetic techniques. The results could also serve as validation to the PSInSAR deformation map. The installation of low-cost GNSS receiver system in the area is to monitor the rate of land subsidence and in the future determine the effectiveness of any mitigation measures. The recognition of the causes of land subsidence is the initial step to mitigating it. Any infrastructure solutions should be built on preparation for the future consequence of allowing the main drivers of land subsidence to continue. Any solutions will fail if the causes are not mitigated. Flooding in the area is usually attributed to rising sea level and clogged drainage but not so much to land subsidence. The small

GNSS receivers or sensors installed in the area are crucial for determining the most effective solutions.

The underlying causes of land subsidence can be due to excessive groundwater pumping and rapid urbanization. In the paper by Rodolfo and Siringan (2006), land subsidence in the area north of Manila, is attributed to excessive groundwater pumping. In the thesis by Maclang et al., (2025), it showed high subsidence rates near high extraction zones from several pumping stations in the delta area. Built-up volume and groundwater withdrawal combined, showed $R^2=0.85$ correlation with land subsidence. Another cause of land subsidence is the natural auto compaction of deltaic sediment (Soria, et al., 2005). However, the small rate of compaction found in the study suggests that human-induced components may account for much of the subsidence in Pampanga (Ibid.). The Mekong Delta is in a similar situation, where excessive groundwater extraction is the main driver of land subsidence (Minderhoud et al., 2017). A 3D numerical model was developed to predict scenarios of land subsidence if groundwater pumping is allowed to continue. Restricting groundwater overexploitation as mitigation measure showed alleviation of land subsidence (Ibid.)

1.2 Geodetic techniques

Geodetic Levelling. This method can achieve a high-level accuracy for vertical control surveying. Differential levelling is a type of geodetic levelling that uses a level and staff to directly measure vertical differences in elevation between two points (NGS, n.d.). The measurements are usually referred from the mean sea level. Although this technique can be classified as highly accurate, but error propagate in long distance. Also, it is a laborious and time-consuming operation. Figure 2 illustrates the method of geodetic levelling.

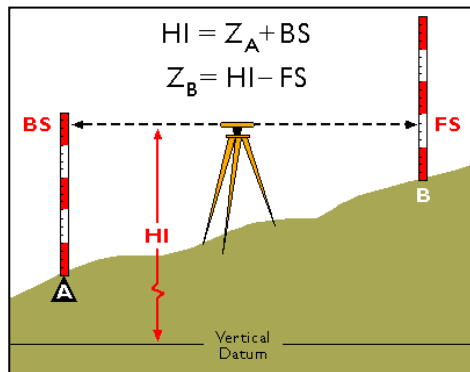


Figure 2. Differential levelling (e-education.psu.edu, n.d.)
 Credit: Adapted from Wolf & Brinker, 1994

In the above figure the elevation at B (Z_B) is determined from a point A with known elevation (Z_A). A level set up midway between two points measures the backsight (BS) on a graduated staff. From this the height of instrument (HI) above s datum e.g. mean sea level (MSL) is determined from the formula given in the figure. Then measuring the foresight (FS) and subtracting it from HI gives the elevation of point B (Z_B). This method is repeated and elevations propagated over for long distances even on a country wide scale.

GNSS levelling. A faster approach to determining height is GNSS positioning. The equation is

$$H = h - N \quad (1)$$

where H is the orthometric height (above the geoid), h is the ellipsoidal height (above the ellipsoid), and N the geoidal undulation. If any two of these quantities are measured, then the third quantity can be computed (Hoffmann-Wellenhoff and Moritz, 2006). The h can be measured easily using a GNSS receiver. However, the accuracy of this technique depends on the accuracy of the geoid used. The orthometric height is treated on this case as approximately equal to height above the mean sea level. Thus, the traditional method of geodetic levelling is superseded by GNSS levelling. Again, this is possible in conjunction with a high-resolution geoid.

2. Method

The framework of the method is as shown in Figure 3. The discussion of each process is detailed in the following sub-sections.

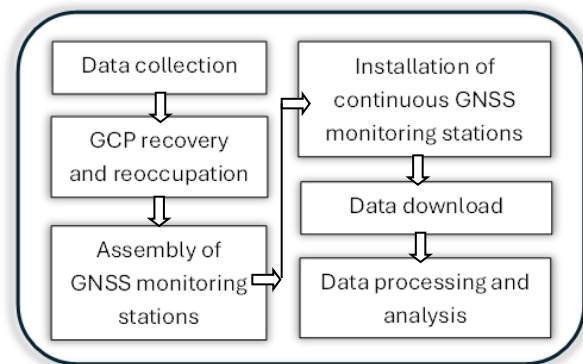


Figure 3. The framework of the method.

2.1 Data collection

The NAMRIA provided 21 benchmarks (BMs) within Hagonoy and Calumpit municipalities. The elevations were determined from a differential levelling conducted in 2021 and 2022. These were new BMs because most of the old ones were already lost. There were only 3 BMs that were recovered and resurveyed located in Guiguinto and Plaridel, Bulacan.

There are 25 ground control points (GCPs) that were also provided by the same agency. These were searched on the ground based on the description in the Point Recovery Form. Majority of these GCPs were observed in 2007 and 2008. The GCPs recovered were re-observed by GNSS receivers.

To monitor the land subsidence occurring in the area, low-cost continuously operating GNSS receivers were installed in the locations listed in Table 1. They were coordinated with the barangays that willingly hosted the stations. The sensor's electrical power was supplied by the local government unit. Most of these were installed in the barangay halls except for Calumpit that was installed near the gate of Sta. Lucia National High School.

| Station ID | Barangay | Municipality | Province |
|------------|---------------|--------------|----------|
| GNT | Poblacion | Guiguinto | Bulacan |
| HGY | Sto. Nino | Hagonoy | Bulacan |
| MCB | Santo Rosario | Macabebe | Pampanga |
| PMR | Pamarawan | Malolos | Bulacan |
| CAL | Sta. Lucia | Calumpit | Bulacan |
| BLT | Balatong | Pulilan | Bulacan |

Table 1. GNSS Monitoring Stations

Figure 4 shows the installation of the GNSS antenna at Sta. Lucia National High School, where most of the time the school were flooded.

The locations of the monitoring stations are shown in Figure 5. The GNSS data can be viewed and downloaded remotely via internet. However, due to weak internet connection, most of the logged data were physically downloaded every 3 months. Efforts are underway to replace the Wi-Fi sticks, which were at first advantageous than pocket mobile Wi-Fi because they are automatically turned-on when connected to the Raspberry Pi Single Board Computers (SBC). This means that every power interruption no manual turning on is necessary when electricity is restored.



Figure 4. Antenna installation at the gate of Sta. Lucia National High School in Calumpit, Bulacan.

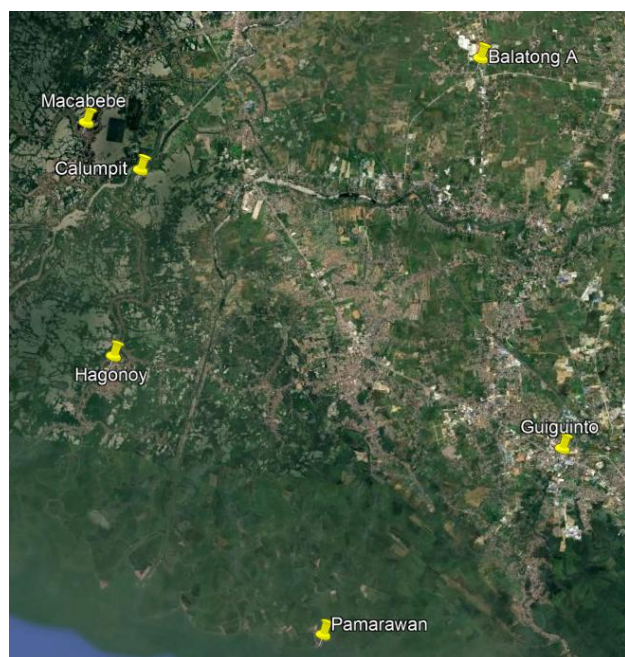


Figure 5. Locations of GNSS monitoring stations.

2.2 GCP Recovery and reoccupation

Despite attempts to recover the GCPs, only 9 were found. Due to frequent construction works to elevate the roads as an immediate solution to the constant flooding, most of these GCPs were lost. The recovered GCPs were then reobserved using GNSS receiver. The data were post-processed using the Active Geodetic Network (AGN) Station in San Rafael, Bulacan (PSRF). New ellipsoidal heights were computed in the recovered GCPs.

2.3 Assembly of continuous GNSS monitoring stations

Using Raspberry Pi SBC the RTKLib software was cloned. A Ublox F9P GNSS receiver was connected to collect signals. Data was logged every 1 sec and file saved every day. This was later re-configured to every 15 sec due to big file size generated. A Wi-Fi stick was connected for checking and remote data access. Most of the time these receivers were just allowed to log.

2.4 Installation of continuous GNSS monitoring stations

The monitoring stations were installed in selected barangays in Bulacan and Pampanga where the rates of land subsidence are high except for Balatong A. Balatong A GNSS receiver was meant as a base station. Its coordinates were determined from PSRF Station. Logging of GNSS signals started for most of these stations last March 2025 except for Pamarawan station that was installed in February. These were meant for long term observations.

2.5 Data download

The logged GNSS data can be downloaded online using Raspi Connect. However, some of these monitoring stations are in places where internet signal is weak or intermittent, therefore physical downloading was necessary.

2.6 Data processing and analysis

For the levelling data a simple comparison was made by just taking the difference between elevations measured from different survey campaigns. The GCPs were re-observed with a GNSS receiver to get new ellipsoidal heights. These heights were compared with the old values, and the rates of change were computed.

The GNSS data from the installed low-cost monitoring stations was post processed using PSRF Station. The observation files from this station were provided by NAMRIA. Daily solutions were computed and graphed. The initial trend of the data was displayed to determine the occurrence of land subsidence.

3. Results

3.1 Results of BM recovery

No benchmarks were re-occupied because of the difficulty of finding a reference benchmarks that are stable. The solution to using these benchmark elevations for quantifying land subsidence is to do new geodetic levelling starting from the nearest tide gauge BM. This is a very tedious job that only the national agency can implement. Another alternative is to re-occupy using GNSS receiver, then assuming that the geoid separation is constant, then orthometric height can be derived. Again, this depends on the BMs that can be recovered. Since most of them are located along the road, then most of them are already lost.

The 21 BMs provided by NAMRIA were newly established BMs, thus no comparison can be inferred. The BMs listed in Table 2 were the only BMs recovered with old levelling elevations from 2018 and new elevations in 2021. The values were differenced to get the change in elevations. The results showed that in 2021 the elevations decreased, which indicate land subsidence.

| BM ID | Location | 2018 (m) | 2021 (m) | Diff. (m) | Rates (mm/yr) |
|--------|-----------|----------|----------|-----------|---------------|
| BL-121 | Guiguinto | 11.45 | 10.67 | 0.78 | -60.09 |
| BL-124 | Plaridel | 8.93 | 8.64 | 0.29 | -22.59 |
| BL-126 | Plaridel | 12.56 | 12.48 | 0.08 | - 5.77 |

Table 2. Comparison of BM elevations

Understandably, BL-121 that is located within the study area has the highest land subsidence rate of -60mm/yr. This is the area where land subsidence is more than 50mm/yr based on the SAR Map. Plaridel on one hand have rates of -10 to -20mm/yr from the same map. These ground measurements just validate the rates derived from SAR images.

3.2 Results of GCP recovery and reoccupation

Out of the 26 GCPs provided by NAMRIA only 9 were recovered and reoccupied. Some of these GCPs were already disturbed and mostly lost. The reason for this is the continuous road elevation works being done in the study area. Obviously, the local government must have to elevate the roads to make them passable so as not to disrupt normal traffic.

The table below (Table 3) is the comparison of average land subsidence velocities derived from nearest Permanent Scatterer Interferometer (PSI) points in the SAR map and GNSS measurements at selected GCPs in Hagonoy and Calumpit.

From just visual inspection there are already obvious discrepancies. BLN 51 and BLN 3062 have more than 70 mm/yr differences. BLN 3072 has around 26 mm/yr difference. The rest ranges from 8 to 16 mm/yr differences. Taking out the outliers (bold text) using 1.5xIQR rule and eliminating difference >20mm/yr, the R² improved to 0.704. As was explained earlier, some of the recovered GCPs have already shown disturbance but these were re-observed anyway because of limited options.

| GCPs | Dist to Nearest PSI Point (m) | Nearest PSI Ave Vert Vel (mm/yr) | GNSS Ave Vert Vel(mm/yr) |
|-----------------|-------------------------------|----------------------------------|--------------------------|
| BLN 14 | 69.613 | -40.446 | -55.060 |
| BLN 15 | 54.454 | -79.468 | -73.712 |
| BLN 51 | 88.856 | -103.229 | -27.722 |
| BL 362 | 7.663 | -89.739 | -76.483 |
| BLN 3062 | 365.940 | -64.883 | -135.000 |
| BLN 3120 | 70.957 | -60.210 | -49.824 |
| BLN 50 | 28.744 | -59.533 | -60.385 |
| BLN 3071 | 41.114 | -52.626 | -60.529 |
| BLN 3072 | 25.886 | -50.890 | -76.588 |

Table 3. Comparison of ground motion vertical velocities.

3.3 Initial results of continuous GNSS monitoring stations

The AGN station in San Rafael, Bulacan (PSRF) was used for post processing the GNSS data from Balatong A, Calumpit, and Guiguinto. Unfortunately, only 12 days of data in February from Pamarawan was post-processed. For some reason the rest of the data until June was only single point positioning. Nevertheless, it was also worth looking into the height trend. The data were mostly from March to May 2025, with data gaps due to brownouts or disruptions due to disturbance of the GNSS receiver. As was mentioned, conclusive results from the monitoring stations can only be had after long years of observations. The results of the processing presented in this paper are only for short period of 3 months.

Figure 6 shows the trend from Balatong A monitoring station. The data was for 36 days (March to April) only. This station was classified in the subsidence map that is less affected by land subsidence. The rate of subsidence based on daily solution is 0.2mm/day.

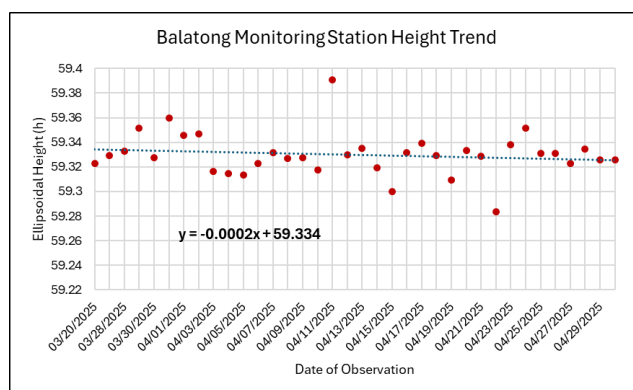


Figure 6. Height (ellipsoidal) trend in Balatong A.

The Calumpit monitoring station in Sta. Lucia National High School has 86 days of observations but with data gaps in the month of April. This was due to disconnection in the power supply. The graph of the daily solution is shown in Figure 7. The computed rate of land subsidence is 1.8mm/day.

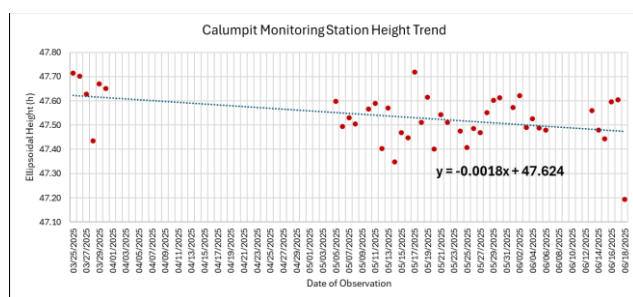


Figure 7. Height (ellipsoidal) trend in Calumpit.

The Guiguinto station is also exhibiting a downtrend in heights which indicate a land subsiding. This was from a data of 46 days from March to May. The rate of land subsidence is computed at 1.2mm/day. Figure 8 shows the graph of the daily solutions.

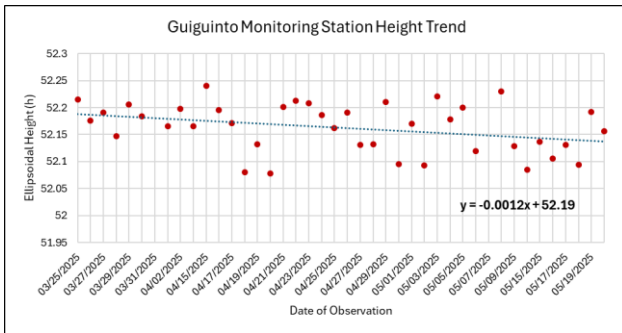


Figure 8. Height (ellipsoidal) trend in Guiguinto.

The Pamarawan monitoring station have 12 days observation that were recovered during the set-up adjustment after 2 weeks from installation. Due to intermittent internet connection this cannot be monitored remotely. It is also difficult to access because Pamarawan can be reached only via a boat ride. Thus, the sensor was just allowed to log. The data was schedule for collection every 3 months. Figure 9a shows the decreasing height from the post processed solution. The rate is around 8.3mm/day. This is high because of short period of observations.

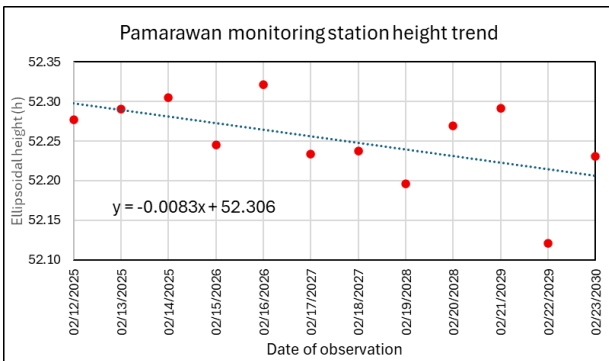


Figure 9a. Height (ellipsoidal) trend in Pamarawan (post processed solution).

The next set of solution for Pamarawan was from single point positioning. The GNSS data collected in June cannot be converted to RINEX format for unknown reasons. There were 105 days of observations from February to June for this solution. Some spurious observations were deleted. Only data within the threshold based on the 1.5*IQR rule considered. Figure 9b shows the height trend from the daily solution. The rate of subsidence for this solution is 3.7mm/day. This is only for checking the height trend and not for accurate quantification of land subsidence.

Unfortunately, Hagonoy station had some power disruptions and there were only few data logged. The Wi-Fi stick in Macabebe station malfunctioned so there was no data transmitted. As of this writing the data gathered for the next batch of processing is from June to August 15, 2025. Due to limited time the results are not yet included in this paper.

Based on the GNSS observations from the different monitoring stations, all the results showed a downward trend in the heights. The data were gathered during the dry season. Interestingly, even for a short period of observations these stations are already showing obvious downtrend except for Balatong A, which is predicted not to be affected by land subsidence. It is worth waiting for the data during the rainy season to see if groundwater recharge is occurring, hence change the trend. Therefore, the

rates presented in this paper are still inconclusive due to limited data.

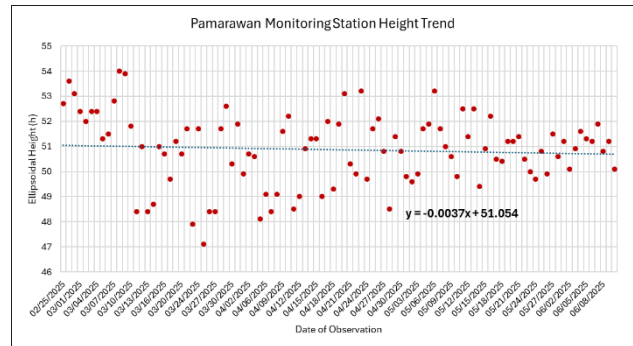


Figure 9b. Height (ellipsoidal) trend in Pamarawan (single point positioning solution).

4. Conclusions

Even though there were few historical geodetic measurements that were recovered in the study area but all of them indicate the occurrence of land subsidence. Actual measurements of road elevations from previous levels agrees with what were computed from geodetic observations. The re-occupation of GCPs showed lower ellipsoidal heights compared with old ellipsoidal heights from NAMRIA observations from 2007/2008.

The installation of GNSS monitoring stations is the best way to monitor land subsidence. It is practical and importantly affordable. The initial processing of GNSS data from monitoring stations in Calumpit, Guiguinto and Pamarawan, indicate land subsidence. For the short period of observations, these are already manifesting downward trends. Balatong A is an area not so much affected by land subsidence as indicated in the SAR map. With rate computed at 0.2mm/day, this could translate to 7.3cm land subsidence in a year. If the rates computed from other stations continues, land subsidence from Calumpit and Guiguinto could amount to 65.7cm and 43.8cm, respectively. Since Pamarawan data was only single point positioning the rate is still not reliable but looking at the trend, this also indicates land subsiding. The rates of lands subsidence based on initial results maybe alarming, however, the incoming data during the rainy season may change the current trend. As these stations are intended for long term observations, hopefully in the coming years they will yield conclusive results.

Acknowledgement

The authors would like to thank PAGeNet of NAMRIA for supporting the research project. Thank you also to Ex-Mayor Angel Lontok Cruz, Lois van der Kleij, Geert Bakker, Dr. Dinesh Manandhar and the LGU officials of Balatong A, Guiguinto, Hagonoy, Macabebe, Pamarawan and the Principal of Sta. Lucia National High School in Calumpit.

References

Casu, F., Manzo, M., Lanari, R., 2006: A quantitative assessment of the SBAS algorithm performance for surface deformation retrieval from DInSAR data. *Remote Sens. Environ.* 2006, 102, 195–210.

Cigna, F., Esquivel Ramirez, R., Tapete, D., 2021: Accuracy of Sentinel-1 PSI and SBAS InSAR Displacement Velocities against GNSS and Geodetic Levelling Monitoring Data. *Remote Sens.* 2021, 13(23), 4800; <https://doi.org/10.3390/rs13234800>

Duan, W., Zhang, H., Wang, C., Tang, Y., 2020: Multi-temporal InSAR parallel processing for Sentinel-1 large-scale surface deformation mapping. *Remote Sens.* 2020, 12, 3749.

European Commission [EC], Joint Research Centre [JRC], 2021: Assessing changes in subsidence rates in the low Pampanga River Basin and Manila Area, Philippines (2021-04-30) (A/2) [Dataset]. European Commission. PID: <http://data.europa.eu/89h/e47cad9f-70c8-4d29-b5d6-d1b89f6ebc9d>

Hofmann-Wellenhof, B., Moritz, H., 2006: *Physical Geodesy* 2nd, corr. ed., SpringerWien New York.

Maclang, JD., Narca, AM., Reyes, R., Mabaquiao, L., 2025: Correlation of land subsidence with groundwater extraction and urbanization in Hagonoy and Calumpit, Bulacan from 2015 to 2021-Q1. Undergraduate Thesis, University of the Philippines Department of Geodetic Engineering.

Minderhoud, P., Erkens G., Pham VH., Bui, VT., Erban, L., Kooi, H., Stouthamer, E., 2017: Impacts of 25 years of groundwater extraction on subsidence in the Mekong delta, Vietnam. *Environ. Res. Lett.* 12 (2017) 064006 <https://doi.org/10.1088/1748-9326/aa7146>

National Geodetic Service (NGS), n.d: <https://geodesy.noaa.gov/heightmod/Leveling/#:~:text=There%20are%20three%20leveling%20techniques,of%20and%20behind%20the%20instrument>

PennState College of Earth and Mineral Sciences, n.d. <https://www.education.psu.edu/natureofgeoinfo/book/export/html/1791>

Reyes, R., Flores, P., Bauzon, A., Alfante, R., Rediang, A., Pasaje, N., 2020: Coastal Sea Level Rise Philippines Technical Report.

Rodolfo, K.S. & Siringan, F.P., 2006: Global sea-level rise is recognised, but flooding from anthropogenic land subsidence is ignored around northern Manila Bay, Philippines. *Disasters*, 30, pp. 118-139.

Soria, JL., Siringan, F., Rodolfo, K., 2005: Compaction rates and paleo-sea levels along the delta complex north of Manila Bay, Luzon Island, Philippines. *Science Diliman (July-December 2005)* 17:2, 39-45.